Egypt. J. Geol., 32, 1-2, (1988): P. 1-25

ON THE GEOLOGY OF THE BASEMENT ROCKS, EAST OF ABU ZENIMA, WEST CENTRAL SINAI, EGYPT.

M.M. EL AREF, M. ABD EL WAHID AND MONA KABESH

Department of Geology, Faculty of Science, Cairo University, Egypt.

Keywords: Migmatites, Schists, Gneisses, Granitoids, Dykes, Geochemistry, Deformation Phases.

The northwestern part of the basement exposure in Sinai is mainly formed of schists, gneisses, migmatites, diorite and old granitoids, intruded by younger pink granites and traversed by sets of dykes of different compositions and trends. Three phases of deformation are recorded in the metamorphic rocks manifested by seven stages of mineral crystallization. Two types of migmatites are recorded, migmatized gneisses exhibiting a stromatic appearance, and higher grade migmatites having banded, boudinage, ophthalmitic and schlieren structures enclosed within the old granitoids. The old granitoids are mainly gneissose and xenolithic. They are calc-alkaline, subduction-related and formed in a compressional environment. Two types of amphibolitic xenoliths are recognized suggesting two parentages. The diorite is found to be more differentiated than the old granitoids, indicating that it was derived from an older highly differentiated magma.

INTRODUCTION

The study area occupies the northwestern extremity of the exposed basement rocks in West Central Sinai, between longitudes 33° 15′ - 33° 27′ E and latitudes 28° 57′ - 29° 5′ 30" N (Fig. 1). Ball (1916) gave few notes on the igneous and metamorphic rocks of this area, but he lumped them as undifferentiated basement on his map. On the geologic map of Sinai constructed from ERTS-1 satellite images (El Shazly *et al.*, 1974), the basement rocks of this area are described

(ISSN 0022-1384)

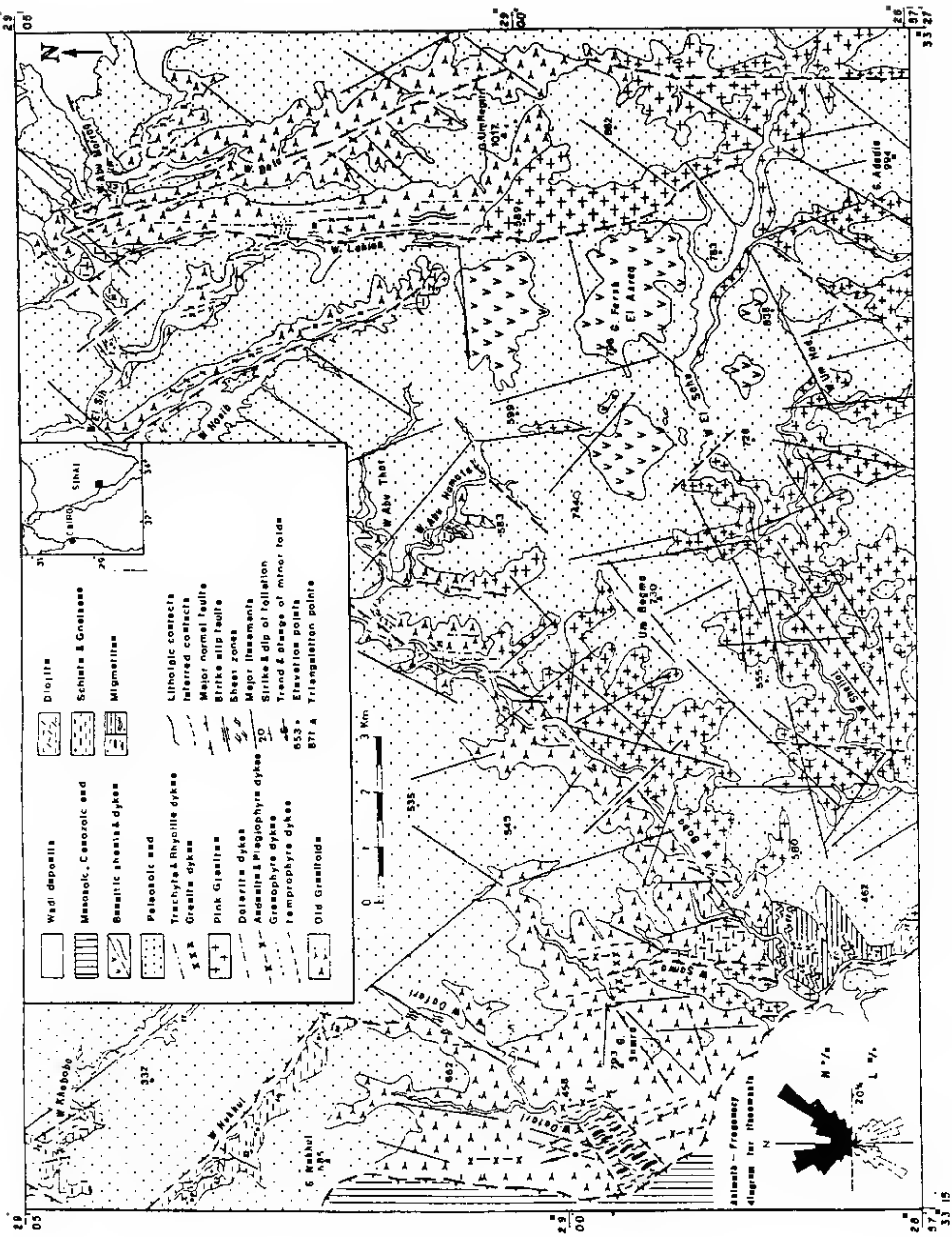
Wadi deposits
Trachyte & Rhyolite dykes
Granite dykes
Pink Granites
Dolerite dykes
Andesite & Plagiophyre dykes
Granophyre dykes
Lamprophyre dykes
Old Granitoids
Diorite
Schists & Gneisses
Migmatites
Lithologic contacts
Inferred contacts
Major normal faults
Strike slip faults
Shear zones
Major lineaments
Strike & dip of foliation
Trend & plunge of minor folds
Elevation points
Triangulation points
3 Km
SINAI
CAIRO
W. Lahian
W. Nasib
W. Abu Thor
W. Abu Hamata
G. Adedia
W. Um Hab
W. Qatar
W. Khabobo
W. Nakhul
G. Nakhul
Azimuth – Frequency diagram for lineaments

as geosynclinal sediments and volcanics, covered by Phanerozoic sediments and lava flows. The present work aims at the discrimination between the different rock units in a chronological order and sheds light on the structural setting. This is approached through mapping of the area using aerial photographs scale 1:40,000, detailed macroscopic and microscopic investigations and geochemical studies of the different rock units.

GEOLOGY

The study area includes the following rock units, arranged from the younger to the older (Fig. 1):

- Basalt sheets and dykes
- Paleozoic sediments (Cambro-Ordovician, Carboniferous)
- Trachyte and rhyolite dykes
- Granite dykes
- Pink granites
- Dolerite dykes
- Andesite and plagiophyre dykes
- Granophyre dykes
- Lamprophyre dykes
- Old granitoids
- Diorite
- Schists and gneisses
- Migmatites

Migmatitic rocks having banded, boudinage, ophthalmitic and schlieren structures enclosed within the old granitoids are recorded in Wadi Dafari. This migmatite exposure is structurally controlled, as it is bounded to the west by a major NNW fault zone and delimited by ENE faults. Migmatized gneisses exhibiting a stromatic appearance are exposed at the southern entrance of Wadi Baba. The schists and gneisses form a belt at the northern part along Wadi El Sih, Wadi Khaboba and Wadi Nukhul, and at the southwestern corner at Wadi Baba. The metamorphic exposures are mainly fault controlled. Diorite forms small masses at the end of

Figure 1. Geologic and structural map of the area east of Abu Zenima, West Central Sinai, Egypt.

Wadi Nasib and the southern entrance of Wadi Baba and Wadi Samra. The old granitoids form the largest exposures in the study area, intruding the schists, diorite and enclosing large rafts of gneisses and migmatized gneisses. The area is traversed by a large number of dykes of different compositions and trends. They are chronologically arranged according to their field relations into: lamprophyric (NW), granophyric (E-W) andesitic and plagiophyric (NNE) and doleritic (NE to NW) dykes. Young pink granites intrude the old granitoids, gneisses and stromatic migmatites. Trachyte and rhyolite dykes cut through the old granitoids and the pink granites. Cambro-Ordovician sandstones (Weissbrod, 1969) overlie the peneplained basement rocks, having a great thickness to the east at Gabal Um Reglin (Pl. 1a) which is reduced to the west. Carboniferous carbonates are represented by a great thickness to the west at Gabal Nukhul and Wadi Khaboba but is reduced to the east. The Cambro-Ordovician units may sharply overlie the paleoerosional surface of the basement rocks, where a typical paleosol profile is developed, or may be marked by basal conglomerate passing upwards to arkose.

Later vulcanicity is represented by the basaltic sheets of El Farsh El Azrag, and basaltic dykes cutting the pink granites, old granites, and the overlying Paleozoic rocks at Um Bogma region and Wadi Lahian.

The rocks present are affected by the main tectonic and structural elements involved in the evolution of the Arabo-Nubian Massif. The main faults traversing the area have NNW and NW trends, other faults and major lineaments have NE, NW

PLATE 1

a: Cambro-Ordovician sandstones overlying the basement at Gabal Um Reglin. b: Biotite gneisa with segregated thin quartz streaks, showing isoclinal folds and cut by quartzofeldspathic veins, Wadi Abu Hamata. c: Photomicrograph of the biotite schist showing the main foliation S1 and a later S3 foliation along the strain cleavage. d: Photomicrograph of a large rounded garnet porphyroblast enclosing oriented elongated quartz and trails of fine opaquea (Si), inclined to the outer foliation (Se). e: Photomicrograph showing a rounded cordierite crystal (crd) enclosing biotite laths parallel to the foliation. Interstitial K-feldspar (light grey) encloses earlier plagioclase, cordierite, biotite and quartz. f: Stretched xenolith, parallel to the foliation of the surrounding granodiorite with formation of plagioclase porphyroblasts. g: Photomirograph of the foliated monzogranite with dark atreaka of biotite and hornblende. h: Photomicrograph of an amphibolitic xenolith, showing large plagioclase porphyroblast enclosing fine hornblende and biotite laths with different orientations, surrounded by fine amphibolitic matrix.

PLATE 1

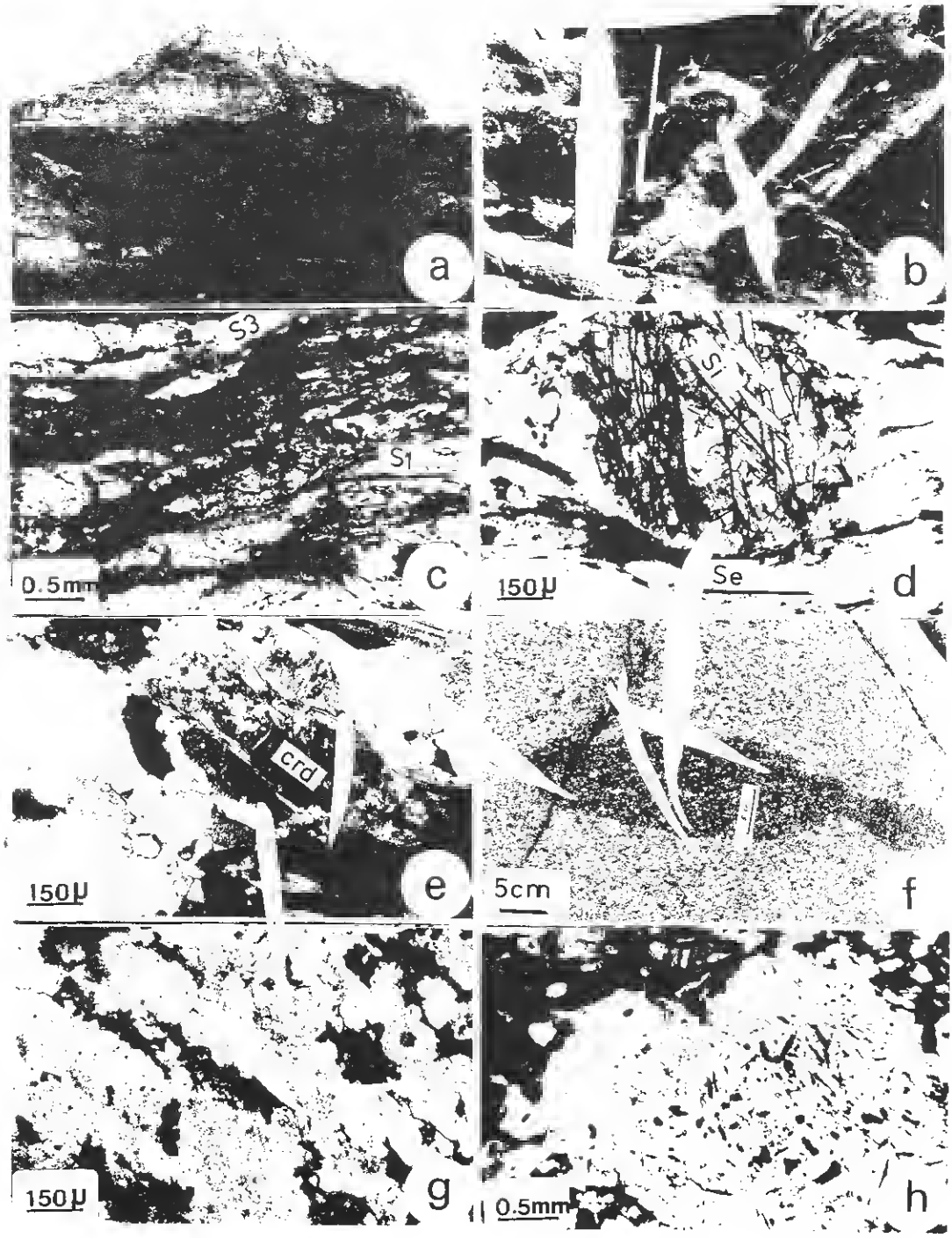

and less frequent E-W trends (Fig. 1). Some of the NW faults are right lateral strike-slip and represent an echo of the strike slip faults of the Gulf of Suez. The major uplift of the area is along a main fault raising the basement rocks against the Miocene and Cretaceous sedimentary rocks at the western border of the area, in cases dragging the Miocene rocks along the contact. Dyke swarms trend parallel to the main structural lines.

1. Migmatites

Two types of migmatites are observed in Wadi Baba and Wadi Dafari. The migmatites of Wadi Baba exhibit well developed stromatic structure and are believed to have developed in a locally closed system by metamorphic differentiation and segregation. On the other hand, the migmatites of Wadi Dafari are of banded, boudinage, ophthalmitic and schlieren types. These migmatites are mainly developed through different degrees of partial melting, affecting different types of parent rocks, and accompanied by brittle and ductile deformation. The fabric evolution, microscopic and geochemical characters and mode of formation of these migmatites are discussed in detail by El Aref *et al.* (1989).

2. Schists and Gneisses

Schists and gneisses form monotonous exposures, that are being structurally controlled. Minor structural elements such as foliation, different types of lineations and minor folds, recorded in these rocks suggest that they have been affected by three main phases of deformation (Pl. 1b and Fig. 2). The first phase of deformation (D_1) is represented by : (a) the main foliation of the rocks S_1, (b) mineral lineation L_1, and (c) the development of segregated thin quartz streaks and lenses parallel to the foliation. The S_1 foliation and L_1 lineation, change their attitude due to later deformation. The second phase (D_2), resulted in : (a) the deformation of S_1 foliation into open symmetric and asymmetric folds and tight isoclinal folds, (b) the development of S_2 axial plane foliation, and (c) formation of L_2 lineation as mineral and crenulation lineation and kinking axes. The third phase of deformation (D_3) is represented by : (a) the formation of a weakly-developed S_3 schistosity as strain slip cleavage, (b) development of irregular

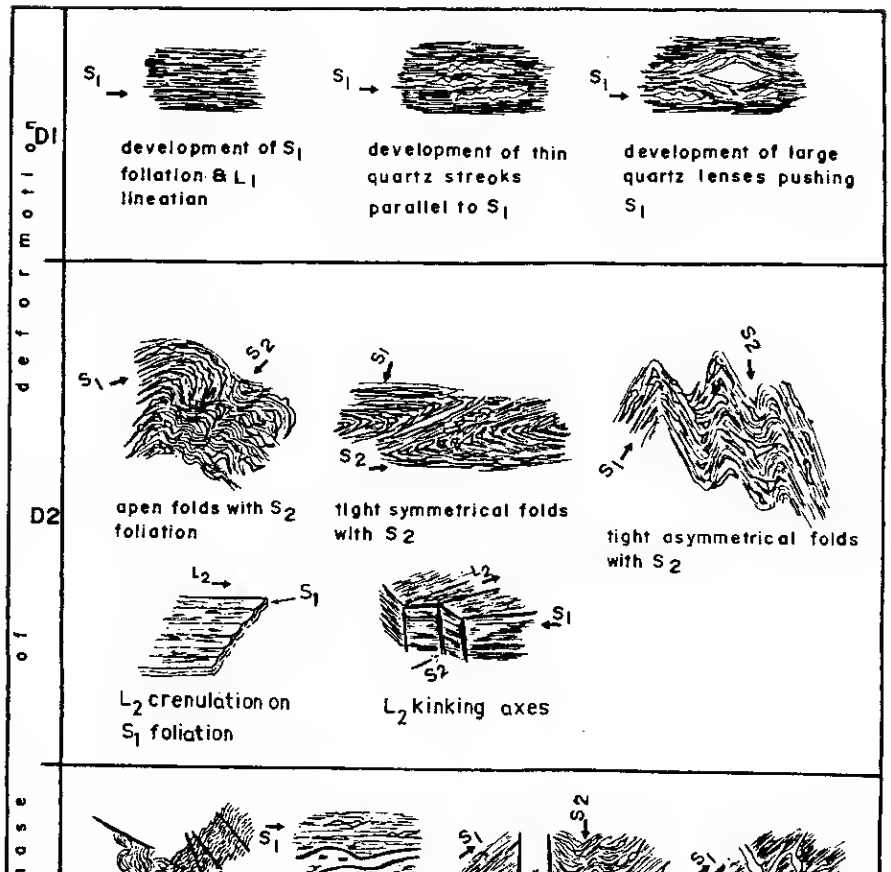

Figure 2. Megascopic features of the schists and gneisses in relation to the deformational phases.

minor folds and kinks near major faults, and (c) the development of granodioritic veins subparallel and cutting the folded gneisses or forming a network of thin veins.

Microscopically, these rocks consist mainly of biotite, plagioclase and quartz. Some varieties contain garnet, cordierite, or a few sillimanite crystals. The main accessories are zircon, apatite and tourmaline. These rocks represent pelitic or semipelitic sediments, metamorphosed up to the lower amphibolite facies. They are divided into the following rock types : (1) Biotite schist, (2) Garnet-biotite schist, (3) Sillimanite - codierite - biotite schist, (4) Garnet-cordierite - biotite schist. (5) Biotite gneiss, and (6) Sillimanite-cordierite-biotite gneiss.

In the different varieties, oriented biotite flakes form the main foliation S_1. Better developed biotites mark the less prominent S_2 foliation. A later phase of biotite as fine highly chloritized flakes are formed parallel to strain slip cleavage S_3 (Pl. 1c). S_1 plagioclase is found as elliptical and oriented untwinned prophyroblasts. They form metablasts enclosing rounded and irregular quartz grains and fine biotite laths. These inclusions may be randomly oriented or arranged with an internal foliation (Si) parallel to the external foliation (Se). The inclusions are mostly randomly distributed within the blasts, or show fine inclusions at the cores and larger quartz and biotite near the margins of the porphyroblasts. Fresh, clear, subhedral plagioclase crystals with prominent lamellar twinning are found parallel to S_2 trend and may enclose larger S_1 biotite flakes. Later plagioclase crystals as post S_2 crystallization, may enclose S_2 biotite flakes.

Garnet is mainly found as large rounded porphyroblasts enclosing oriented, rounded and elongated quartz crystals, with an internal foliation Si inclined to the external foliation Se (Pl. 1d), indicating post crystallization rotation of the garnet porphyroblasts. Syntectonic growth of garnet is represented by idiomorphic crystals with fine slender inclusions arranged in a spiral pattern, indicating rotation during crystal growth. Post-kinematic garnet crystals, show irregular intergranular blastic growth enclosing quartz crystals similar to the surrounding matrix. Later small rounded garnet crystals overprint S_2 biotite flakes.

Cordierite forms small xenoblastic lenticular crystals mainly associated with biotite, or may coalesce together forming streaks controlled by the main schistosity. Large xenomorphic elliptical cordierite forms metablasts enclosing biotite and quartz crystals (Pl. 1e). The cordierite crystals are highly altered (pinitized) to fine sericite and chlorite aggregates. Some crystals include yellow to orange irregular patches of an isotopic amorphous substance with a glassy appearance.

Sillimanite is mainly found as fine fibrous aggregates associated with S_1 biotite flakes.

The gneisses are medium to coarse grained with well developed foliation and segregation. Plagioclase is found as xenomorphic crystals stretched along the foliation and enclosing fine biotite and quartz, or as subidiomorphic crystals with albite twinning. Some rocks show segregation of dark selvages of foliated biotite and cordierite melanosomes alternating with coarse grained quartzofeldspathic leucosomes with biotite flakes and large rounded cordierite crystals. Later K-feldspar crystallizes as anhedral interstitial crystals, enclosing and partly corroding earlier crystals (Pl. 1e).

The microtextural and microstructural evolution of the metamorphic assemblages with respect to the detected three phases of deformation and the stages of crystallization is illustrated in Figure 3.

3. Diorite

Dark dioritic to quartz dioritic rocks form masses at Wadi Baba, Wadi Samra and Wadi Nasib, surrounded and cut by old granitoids. They are highly weathered and epidotized. The dioritic rocks are medium to coarse grained with subhedral twinned plagioclase crystals, mostly zoned. Some rocks are affected by low grade metamorphism resulting in the formation of actinolite, chlorite and epidote. Quartz diorites show hypidiomorphic to panidiomorphic eguigranular or porphyritic texture with interstitial quartz.

4. Old Granitoids

The western exposures of these old granitoid rocks form high mountains, while to the east they exhibit low to moderate relief with spheroidal weathering. They are

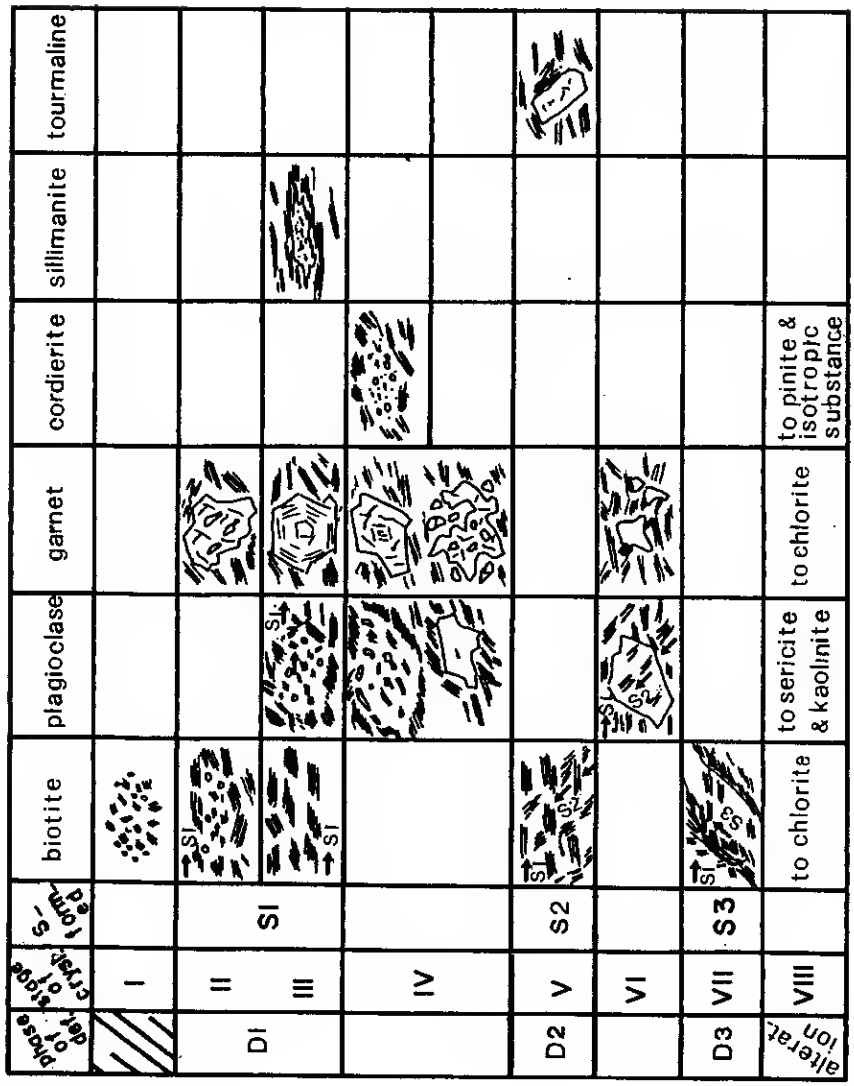

Figure 3. Microtextural and microstructural evolution of the metamorphic assemblages.

weakly to moderately foliated and occasionally show two foliation trends. They have intrusive contacts against the schists and diorites, and send apophyses cutting the older diorite masses and enclose diorite rafts. Near the contacts with the schists they are foliated parallel to the main foliation S_1 in the schists, suggesting a late D_1 intrusion of these granitoids. The granitoids commonly enclose dark enclaves distributed throughout the whole mass and may cluster near the peripheries, at the entrance of Wadi Baba and Wadi Lahian. These enclaves are mostly fine to medium grained, of dioritic and amphibolitic composition and have sharp contacts with the old granitoids. They are stretched and foliated parallel to the main foliation of the granitoids (Pl. 1f). In cases, the two foliation trends recorded in the granitoids are also observed in the xenoliths, proving the secondary origin of these foliations. The xenoliths may be twisted or folded or sharply cut and displaced by minor faults. At Wadi Dafari, the enclaves are recorded in swarms, parallel to the granitoid foliation and are being locally invaded by granodioritic veins. Most enclaves are affected by the enclosing granodiorites and are texturally and mineralogically modified. The trasformation starts with the formation of large plagioclase propyroblasts and hornblende crystals oriented parallel to the outer foliation (Pl. 1f). This is accompanied by coarsening of the matrix, that progressively reaches the same size as the enclosing old granitoids. These modifications result in coarser lighter cores and finer darker outer margins. They appear to having been initiated through the thermal and possible metasomatic effects of the granodiorite.

Petrographically, the old granitoids and associated rock varieties are classified into the following rock type : (1) Old granitoids (monzogranite, granodiorite, tonalite, monzodiorite and monzonites) and (2) Dark xenoliths (diorite, microquartz diorite, and amphibolite).

The granitoid rocks show textural variations due to the degree of foliation and mineral morphology. The monzogranites are well foliated (Pl. 1g), and show anhedral to subhedral plagioclase, mostly untwinned and enclose fine biotite, hornblende and quartz crystals. Potash feldspars crystallize as later interstitial crystalloblasts. The mafics form irregular dark streaks

of oriented biotite flakes, and blastic hornblende enclosing quartz and plagioclase, or hornblende aggregates surrounded by biotite.

The granodiorites, show homogenization of the rock fabric with a less developed foliation, and an increase in the degree of idomorphism of plagioclase and hornblende. Plagioclase forms subhedral to euhedral crystals, twinned and mostly zoned. They show simple zoning and oscillatory zonal growth with poorly defined to sharp zones. Potash feldspars grow intergranularly and may partly or completely enclose earlier crystals. Hornblende forms subhedral to euhedral crystals, or shows large crystals enclosing quartz and plagioclase.

The tonalite shows well developed foliation, with oriented subhedral plagioclase displaying albite lamellar twinning and hornblende as subhedral crystals that may enclose quartz and plagioclase. The described rocks are affected by deformation, showing bending of plagioclase crystals, with twisted, wedged or abruptly terminated twin lamellae, occasionally affected by microfaults. Biotite flakes are bent, kinked and show wavy extinction. Quartz crystals show undulose extinction, and higher plastic deformation due to the squeezing of quartz between the plagioclase and the mafics.

The monzodiorites have lower quartz content than granodiorites and higher K-feldspars than the tonalites. They show hypidiomorphic granular texture, with subhedral, zoned and twinned plagioclase, subhedral biotite and hornblende and anhedral interstitial orthoclase and microperthite. The K-feldspars partly or completely enclose and corrode earlier crystals.

Monzonite is a more alkaline variety consisting of anhedral orthoclase and microcline perthite enclosing plagioclase and biotite, with a few quartz crystals.

In the dark xenoliths, the diorite variety is weakly foliated, and modified by the blastic growth of plagioclase and hornblende. The micro-quartz diorite shows porphyritic and doleritic textures. The amphibolitic xenoliths are fine grained, foliated and consist of hornblende, plagioclase and some biotite. They are commonly modified by large plagioclase porphyroblasts having euhedral cores packed with fine rounded hornblende and biotite laths and clear outer

margins (Pl. 1h) or enclose small plagioclase and coarser hornblende crystals at the outer zone. Later plagioclase porphyroblasts show irregular boundaries with clear cores and fine inclusions distributed at the interzonal phases.

5. Dykes and pink granites

Dykes of variable composition and age traverse the area in different directions. The old dykes of lamprophyric, andesitic, plagiophyric and doleritic compositions cut the different varieties of the basement rocks except the pink granites which are cut only by later trachyte and rhyolite dykes. Granite dykes, most probably related to the late magmatic phase of the pink granite intrusion, cut the old granitoids and the andesite dykes of Wadi Samra. Later basaltic dykes cut across the basement rocks and the overlying Cambro-Ordovician and Carboniferous sedimentary rocks.

The lamprophyric dykes include two varieties, spessartite and camptonite. The former consists of microlithic needles of green hornblende and sericitized plagioclase laths, in cases, forming phenocrysts. The latter camptonite dykes consist of plagioclase and alkali-iron amphibole (barkevikite), showing fine to medium grained and porphyritic varieties and may contain stumpy and acicular tremolite associated with chlorite patches. The granophyre is composed of sodic plagioclase phenocrysts and a few biotite, surrounded by fine plagioclase laths, quartz, and orthoclase showing granophyric texture. The andesite dykes consist of euhedral plagioclase (andesine) phenocrysts mostly zoned, embedded in a medium grained matrix of plagioclase, biotite and hornblende. A variety shows barkevikite phenocrysts. The plagiophyre dykes consist of plagioclase phenocrysts, green biotite and brown hornblende in a fine grained matrix with abundant K-feldspars exhibiting a granophyric texture. Dolerite dykes are formed of fine to medium grained plagioclase and interstitial hornblende and titanaugite, with highly altered olivine crystals, exhibiting doleritic, ophitic and subophitic textures.

The last main magmatic event in the area is represented by the late, anorogenic pink granites, corresponding to the second and third group of El Gaby (1975), Abu-El Liel (1980) and Hussien *et al.*, (1982).

The pink granite mass that occupies the southeastern part of the area, sharply intrudes the old granitoids and the gneisses along Wadi Baba, Wadi Samra, Wadi Budra and Wadi Lahian. The pink granites are commonly coarse grained, formed of large stained K-feldspars, quartz and minor decomposed biotite. They are, in cases, fine grained or porphyritic with large K-feldspar phenocrysts. They include veins and pockets of pegmatites.

Petrographically, they are either normal granites or perthite granites. The normal granites show euhedral to subhedral plagioclase, and subhedral to anhedral crystals of flame and patch perthite. The porphyritic variety shows large perthite megablasts, up to 5 mm in diameter, enclosing quartz, plagioclase and biotite flakes. The perthite granite consists mainly of large crystals of flame perthite that are commonly stained. Some perthites enclose cuneifrom and vermicular quartz, or are corroded and penetrated by quartz.

The granite dykes are coarse grained, and are made up of sodic plagioclase, perthite, guartz and a few biotite crystals. The rhyolite dykes show euhedral guartz and perthite phenocrysts embedded in a fine grained quartzofeldspathic matrix. The trachyte dykes are composed of euhedral fine orthoclase, some may contain plagioclase phenocrysts.

The basalt dykes consist of plagioclase phenocrysts in a fine matrix of plagioclase and altered mafics, that may show doleritic texture or contain amygdales filled by secondary chlorite and zeolite.

GEOCHEMISTRY

Ten representative samples of the old granitoids and the associated diorite and amphibolite xenoliths were chemically analysed (Table 1), some migmatitic leucosomes of schlieren type are considered for comparison. Some element relations and computations are carried out, as Niggli Values and normative composition (Tables 1 and 2). The used variation diagrams portary the chemical characteristics and discriminate between the different varieties or indicate the stage of differentiation, magma type and tectonic setting of the old granitoids.

The general trend of the chemical analyses of the granitoid rocks ranges from granodiorite, with slightly higher K_2O content, to adamellite, with higher CaO content than the averages of Le Maitre (1976). The old granitoids and associated diorites fall in the calc-alkaline field of Wrights' alkalinity ratio diagram (Fig. 4a), whereas the migmatite leucosomes show an alkaline tendency with higher SiO_2 and alkalies. In Figure 4b, the old granites fall in the calc-alkalic batholiths field related to subduction zone of Rogers and Greenberg (1981). On the AFM diagram of Petro *et al.* (1979) (Fig. 4c), the present old granitoids plot near the curve perpendicular to the FM-side, indicating a compressional environment. Figure 4d, shows that the calc/alkali index of the granitoids is 60, indicating a compressional suite. On the al-alk diagram (Fig. 5a), the old granitoids and diorites are relatively alkali rich. On the al-fm diagram (Fig. 5b) the old granitoids show a salic character, while the diorites have a semi-salic character. This Figure shows a clear discrimination of two types of amphibolite xenoliths. On the chemical classification diagram of Streckeisen (1976) based on the Or-Ab-An normative contents (Fig. 6), the old granitoids fall in the monzogranite field, while the migmatitic leucosomes plot separately in the alkali granite field. In Figure 7, the old granitoids fall in the plagioclase field near the two-feldspar boundary curve of James and Hamilton (1972); whereas the granitic migmatitic leucosomes fall within the thermal trough and mostly coincide with the area of highest concentration of granitic melts of Tuttle and Bowen (1958). Plotting of the normative Qz-Or-Ab values on the H_2O saturated liquidus field boundaries of Tuttle and Bowen (1958) and Luth *et al.* (1964) (Fig. 8) shows that the old granitoids fall at moderate to high water vapour pressure, indicating that they were possibly formed at deep levels of the crust.

On the Ba-Rb-Sr diagram (Fig. 9) (after El Bouseily and El Sokkary, 1975), the old granitoids fall in the granodiorites and anomalous granite fields, with relatively higher Sr and increasing Ba contents. The diorite plots in a position indicating that it is even more differentiated than the old granitoids. This proves that the diorite belongs to an older highly differentiated magma of different parentage than the granodiorites. The migmatitic leucosomes fall in the normal granite field having a higher position in the proposed differentiation trend.

Table 1. Chemical analyses of the old granitoids, diorites, amphibolite xenoliths and some migmatite leucosomes.

	Old Granitoids							Dio-rite	Amphibolite xenoliths		Migmatite leucosomes			
Sample No.	L 19	BL 6	S1	H_2O	B4	D 101	D	N3	BL 5	D1	a	b2	S1	S2
SiO_2	66.02	66.40	65.85	65.12	68.61	63.94	61.13	59.42	51.71	51.05	70.13	73.06	71.63	72.10
Al_2O_2	14.93	14.71	14.70	15.30	15.12	15.79	16.22	15.53	15.62	12.49	13.58	13.86	13.54	13.09
Fe_2O_3	2.44	0.20	2.35	2.55	0.95	1.88	2.55	5.01	6.81	5.99	1.20	0.15	1.84	0.83
FeO	1.12	2.79	1.39	1.12	0.84	1.67	1.67	2.65	2.79	4.19	0.70	0.84	0.81	1.12
MgO	1.35	1.86	1.03	1.83	1.12	1.80	2.27	1.98	2.27	8.41	1.66	0.23	0.66	0.74
K_2O	4.02	4.11	4.04	4.05	4.03	4.06	4.24	4.13	4.51	4.25	4.57	4.59	4.19	4.43
Na_2O	3.72	4.00	4.49	4.63	5.23	4.81	4.96	5.45	6.72	5.00	5.13	5.03	4.13	5.25
CaO	3.41	3.22	3.29	3.07	1.89	3.21	3.43	3.17	7.52	6.91	1.12	0.77	1.65	0.95
TiO_2	0.54	0.33	0.55	0.31	0.28	0.70	0.92	0.89	0.30	0.25	0.46	0.29	0.43	0.26
MnO	0.05	0.12	0.06	0.08	0.03	0.06	0.08	0.10	0.15	0.17	0.05	0.03	0.04	0.04
P_2O_5	0.54	0.29	0.66	0.23	0.49	0.28	0.67	0.19	0.77	0.46	0.19	0.00	0.03	0.07
Total	98.41	98.03	98.41	98.29	98.59	98.20	98.14	98.52	99.17	99.17	98.79	98.85	98.25	98.87
Rb	269.00	241.90	282.40	276.60	245.20	269.10	276.80	287.40	271.40	315.60	208.40	284.40	266.50	239.10
Sr	499.70	534.80	417.90	563.20	356.20	661.30	609.60	613.90	1077.0	655.30	489.30	459.40	484.50	478.90
Y	19.20	31.80	19.20	19.20	19.20	29.20	51.70	76.80	21.30	19.20	119.60	19.20	49.00	71.30
Zr	71.20	230.80	55.20	184.90	67.80	178.80	256.40	293.90	309.0	246.0	488.10	405.0	232.90	550.50
Ba	1462.0	17119.10	661.80	1766.0	939.50	986.10	725.50	2015.40	183.70	0.00	5480.20	3275.00	3432.4	2753.0
La	70.80	72.60	94.50	35.80	69.90	37.00	36.00	38.00	131.40	262.00	55.80	41.60	55.40	38.20
Nd	0.00	20.20	0.00	13.30	21.00	0.00	14.60	53.50	38.70	0.00	16.40	0.00	0.00	0.00
Pb	86.30	67.90	1.60	64.90	10.90	45.00	9.40	83.30	58.30	79.90	86.10	32.30	58.70	61.00
Th	21.80	73.40	43.10	130.70	6.90	94.10	139.00	121.30	83.80	44.40	45.30	0.50	14.00	7.30
U	0.20	0.00	0.20	0.30	0.10	0.20	0.00	0.30	18.50	2.20	44.10	0.20	0.00	0.00
Qz	21.55	16.98	17.68	14.70	17.67	12.24	8.02	3.21	--	--	17.95	22.58	26.44	20.69
Or	24.35	24.75	24.50	24.00	23.95	24.25	25.30	24.70	--	--	27.10	27.35	25.50	26.35
Ab	34.20	36.50	41.00	42.00	47.10	43.6	44.90	49.40	--	--	46.15	45.50	37.85	47.30
An	6.87	7.30	6.10	7.00	3.12	7.12	6.40	5.70	--	--	0.00	1.92	4.10	0.00

L 19 = Gneissose tonalite
S 1 = Monzogranite
B 4 = Granodiorite
D = Monzonite
BL 6 = Gneissose tonalite
H20 = Sillimanite bearing granodiorite
D 101 = Monzodiorite
N 3 = Diorite
D1, BL5 = Amphibolite xenoliths
a = Leuc., banded type
b2 = Leuc., around boudin
S1 = Leuc., schlieren type
S2 = Leuc., schlieren type

Symbols used in the plottings,

Granodiorite ✕ Diorite △ Amphibolite ■

Migmatite Leucosomes O

Table 2. Niggli values for the old granitoids, diorite and amphibolite xenoliths.

SP. No.	L 19	BL6	S1	H2O	B4	D 101	D	N3	BL5	D1
al	037.49	036.11	036.60	035.98	041.60	036.39	0.34.66	031.00	024.40	017.07
fm	020.60	022.39	019.12	022.60	013.15	021.75	024.65	030.61	029.17	048.19
c	015.59	014.40	014.90	013.14	009.48	013.47	013.37	011.50	021.40	017.20
alk	026.30	027.09	029.32	028.25	035.74	028.39	027.31	026.85	024.90	017.54
Si	281.77	277.10	278.90	260.36	321.20	250.50	222.40	201.70	137.60	118.60
K	000.41	000.40	000.37	000.36	000.34	000.36	000.36	000.33	000.30	000.36
mg	000.42	000.52	000.34	000.48	000.49	000.48	000.50	000.33	000.31	000.61
qz	076.57	068.74	061.60	047.36	078.26	036.95	013.17	-5.71	-60.50	-50.15

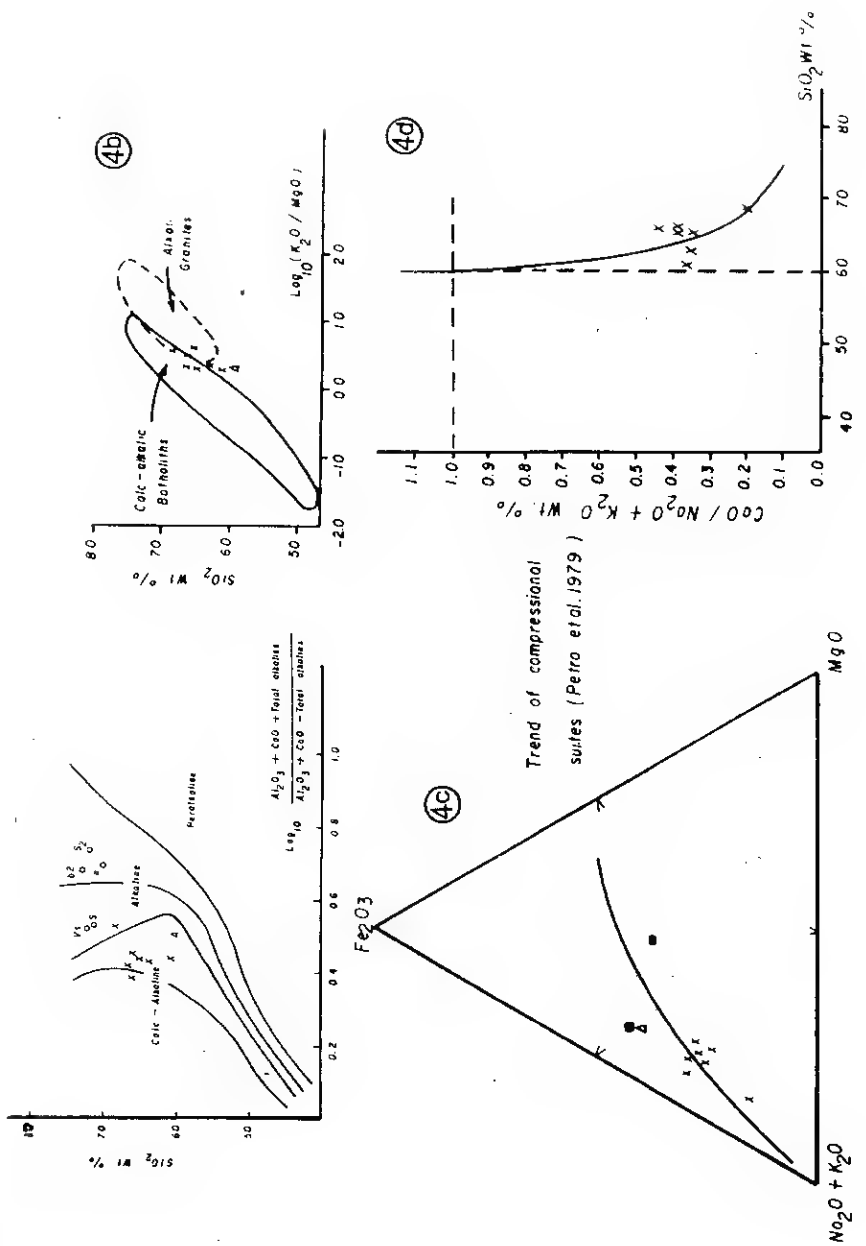
4a
Peralkaline
Alkaline
Calc - Alkaline
Sub-alkaline
4b
Calc - alkalic Batholiths
Alkali Granites
4c
Trend of compressional suites (Petro et al. 1979)
Fe2O3
MgO
Na2O + K2O
4d
SiO2 Wt %

SUMMARY AND CONCLUSIONS

The area of study was mapped using aerial photographs (scale 1:40,000) and the different rock units were discriminated. Their field relations, macroscopic, microscopic and geochemical characters throw much light on the geologic setting, phases of deformation and the magma types.

Two types of migmatites are recognized in the studied area, namely: migmatite having banded, boudinage, ophthalmitic and schlieren structures and stromatic (metamorphic) migmatite.

The schist and gneiss exposures are mainly fault controlled. They represent essentially pelitic or semipelitic sediments, metamorphosed up to the amphibolite facies. The minor structural elements of the schists and gneisses, suggest that they were affected by three main phases of deformation. The microtextural and microstructural evolution of the metamorphic assemblages clarifies the stages of crystallization related to the observed three deformational phases. The S_1 foliation is mainly represented by preferred oriented biotite and quartz crystals. It is characterized by pronounced blastic growth of plagioclase as elliptical poikiloblasts, marking the metablastasis stage of development of the metamorphic rocks, with growth of granet poikiloblasts in some varieties. Oriented biotite flakes and some plagioclase mark the less prominent S_2 foliation, occasionally overprinted by S_3 strain-slip cleavage.

The granitoids are mostly xenolithic and foliated. The dark xenoliths are dioritic and amphibolitic in composition,

---

Figure 4. a: Wright' alkalinity ratio diagram, for the old granitoids and the migmatite leucosomes (Wright, 1969). b: SiO_2 versus Log10 (K_2O/MgO) plot, after Rogers and Greenberg (1981). c: AFM diagram, the curve shows the trend proposed by Petro *et al*, (1979) for compressional suites. d: Variation diagram of CaO/Na_2O + K_2O versus SiO_2. Calc/Alkali index is 60 (after Petro *et al*, 1979)

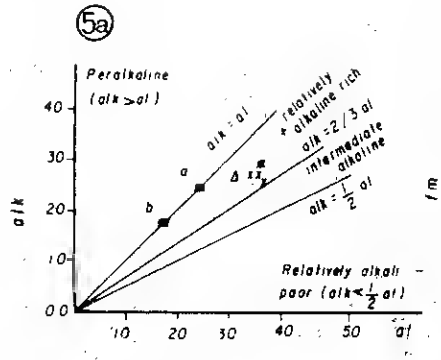

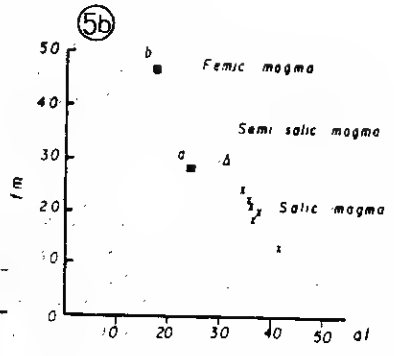

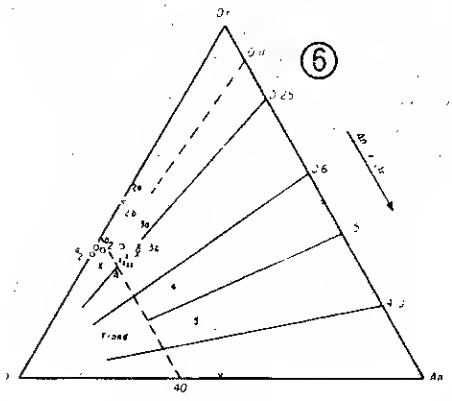

(2a) ALKALI GRANITE
(2b) ALKALI - FELDSPAR GRANITE
(3a) SYENO - GRANITE
(3b) MONZO - GRANITE
(4) GRANODIORITE
(5) TONALITE TRONDHJEMITE

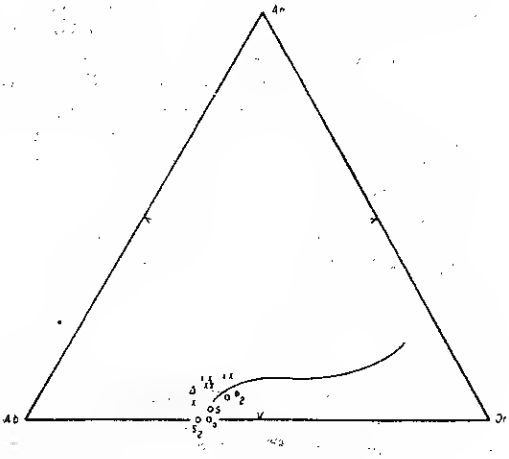

stretched and foliated parallel to the outer foliation of the old granitoids. The amphibolite xenoliths are texturally and mineralogically modified by the formation of large plagioclase and hornblende porphyroblasts. Compositionally, the old granitoids range from tonalite and monzodiorite to granodiorite and monzogranite. They are intruded by the pink granites. Accordingly, the rocks are mainly considered as "old", "grey", "synorogenic" granite corresponding to G_1-granite of Hussein *et al.* (1982). Plotting of the analyses of the old granitoids, diorite and amphibolite xenoliths on different variation diagrams, clearly discriminates between them, some even separate between two types of amphibolite xenoliths, suggesting two different parentages. The diorite is believed to have been derived from an older highly differentiated magma. The old granitoids are found to be calc-alkaline, related to a subduction zone and a compressional environment, being formed by partial melting of the lower crust. From the field relations and petrographic characteristics, the pink granites correspond to the G_2 granite type.

The dyke swarms represent the limit of the Pan-African compression event and mark the post-tectonic extensional phase. These dykes cut the different basement rock units. Younger basaltic dykes cut the basement rocks and the overlying Cambro-Ordovician and Carboniferous sedimentary succession. The young dykes belong to the late Paleozoic to Mesozoic volcanic activity of Sinai.

Figure 5. a: Plot of al-alk after Burri and Niggli (1945). b: Plot of al-fm diagram of Niggli (after Burri, 1959).

Figure 6. Classification scheme of granitic rocks (after Streckeisen, 1976).

Figure 7. Normative Or-Ab-An proportions for the granitoids. The solid line represents the two feldspar boundary for the quartz saturated ternary feldspar system at 1000 bars water-vapour pressure(after James and Hamilton, 1972).

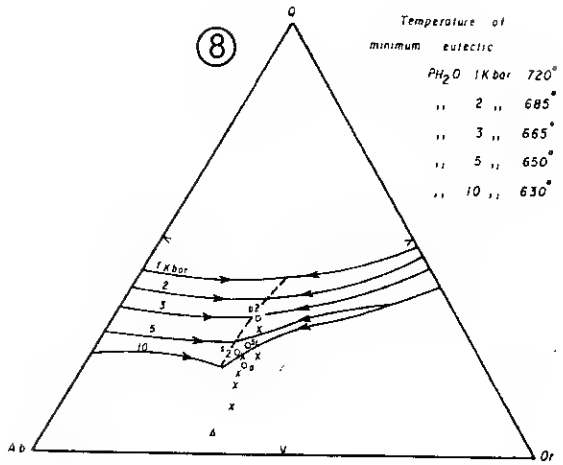

Figure 8. H_2O Saturated Liquidus field boundaries in the system Qz-Ab-Or-H_2O for different water pressures 1,2,3, K bar (after Tuttle and Bowen, 1958), 5, 10, K bar (after Luth *et al*, 1964). The dashed line is the trace of the isobaric minima of the granitic system.

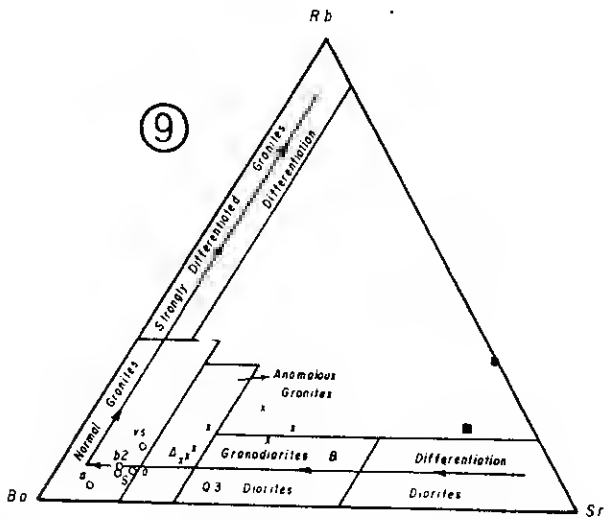

Figure 9. Ba-Rb-Sr ternary diagram for the studied rocks (El-Bouseily and El-Sokkary, 1975).

ACKNOWLEDGEMENTS

The authors wish to express their deep thanks to Prof. M.A. El-Sharkawy for his fruitful discussions and assisting in carrying out the chemical analysis of the samples in the laboratories of the Kuwait University.

REFERENCES

Abu El Leil, I. (1980) "Geology, petrography and geochemistry of some granitic rocks in the northern part of the basement complex, Egypt". Unpub. Ph.D. Thesis, Al-Azhar University.

Ball, J. (1916) "Geography and geology of West Central Sinai, Egypt". Surv. Dept., Cairo, 219 P.

Burri, C. (1959) "Petrochemische Berechnungsmethoden auf agrivalenter Grundlage". Verlag Birkhauser, Basel.

Burri, C. and Niggli, P. (1945) "Die Jungen Eruptivgesteine des mediterqnen Orogens ". 1. Publi. Vulkanistitut Immaneul Friedlander, No. 3.

El Aref, M.M., Abd El Wahid, M. and Kabesh, Mona (1989) "Fabric evolution and geochemical characters of the gneisses and migmatites of Wadi Baba and Wadi Dafari, West Central Sinai, Egypt". Egypt. Mineral. Soc., Vol. 1, P. 26-53..

El Bouseily, A.M. and El Sokkary, A.A. (1975) "The relation between Rb, Ba and Sr in granitic rocks". Chem. Geol., Vol. 16, P. 207-219.

El Gaby, S. (1975) "Petrochemistry and geochemistry of some granites form Egypt". Neues. Jb. Miner. Abh. 124, P. 147-189

El Shazly, E.M., Abdel Hady, M.A., El Ghawaby, M.A., El Kassas, I.A. and El Shazly, M.M. (1974) "Geology of Sinai Peninsula from ERTS-1 satellite images". Remote Sensing Research Project, Academy of Scientific Research and Technology, Cairo, Egypt.

Hussein, A.A., Aly, M.M. and El Ramly, M.F. (1982) "A proposed new classification of the granites of Egypt". J. Volcan. and Geother. Research., Vol 14, P. 187-198.

James, R.S. and Hamitton, D.L. (1972) "Phase relation in the system $NaAl-Si_3O_8-K\ Al\ Si_3O_8-CaAl_2\ Si_2O_8$ at 1 Kilobar water vapour pressure". Contr. Mineral. Petrol., Vol. 21, P. 111-141.

Le Maitre, P.W. (1976) "The chemical variability of some common igenous rocks". J. Geol., Vol. 17, No. 4, P. 589-637.

Luth, W.C., Janns, R.H. and Tuttle, O.F. (1964) "The granite system at pressure of 4 to 10 Kilobars". J. Geophys. Res., Vol. 69, P. 759-773.

Petro, W.L., Vogel, T.A. and Wilbad, J.T. (1979) "Major element geochemistry of plutonic rock suites from compressional and extensional plate boundaries". Chem. Geol., Vol. 26, P. 217-235.

Rogers, J.J.W. and Greenberg, J.K. (1981) "Trace elements in continental margin magmatism". Part III: "Alkali granites and their relationship to cratonization." Geol.Soc. Amer. Bull. Part 1, Vol, 92, Nos. 4-6 and Part II, Vol. 92, P. 57-93.

Streckeisen, A. (1976) "To each plutonic rock its proper name". Earth Sci. Rev., Vol. 12, P. 1-33.

Tuttle, O.F. and Bowen, N.L. (1958) "Origin of granite in the light of experimental studies in the system $NaAl\ Si_3O_8-K\ Al\ Si_3\ O_8-SiO_2-H_2O$". Geol. Soc. Am. Mem., No. 74, 153 P.

Weissbrod, T. (1969) "The Paleozoic of Israel and adjacent countries". (Part 2), The Paleozoic outcrops of Southwestern Sinai and their correlations with those of Southern Israel. Geol. Surv. Israel, Vol. 48, 32 P.

جيولوجية المعقدة القاعية للمنطقة شرق أبو زنيمة، غرب وسط سيناء، مصر

مرتضى مراد العارف، محمد عبد الواحد ،
ومنى كابش
قسم الجيولوجيا ، كلية العلوم، جامعة القاهرة-الجيزة

تشتمل المعقدة القاعية فى المنطقة شرق أبو زنيمة، بغرب وسط سيناء على صخور الشست والنيس والمجماتيت والديوريت وصخور جرانيتية قديمة. تداخلتها صخور الجرانيت الوردى وتقطعها مجموعات من الفواطع مختلفة التركيب والاتجاه والعمر.

وقد دلت الدراسة على أن صخور النيس والشست قد تعرضت لثلاث مراحل أساسية من التشوه مصحوبة بسبع فترات من التبلور المعدنى.

ويناقش البحث تفصيلا الخواص الكيميائية والبتروجرافية للصخور الجرانيتية القديمة والديوريت وبعض أنواع من المجماتيت،ثم يستنتج أن صخور الديوريت قد تكونت من صهارة أقدم من تلك التى كونت الصخور الجرانيتية القديمة. كما أمكن الاستدلال على بيئة تكون هذه الصخورالجرانيتية القديمة.